OPEN ACCESS Freely available online

IJCMB
International Journal of Clinical Medicine and Bioengineering

ISSN 2737-534X
Volume 2, Issue 1
https://www.iikii.com.sg/journal/IJCMB
International Journal of Clinical Medicine and Bioengineering

Article

Ordinal Pattern-Based Dissimilarity Measure for Slow Cortical Potential Training in Stroke

Wenbin Shi *, Chuting Zhang, Chien-Hung Yeh and Heng Liu *

School of Information and Electronics, Beijing Institute of Technology, Beijing, China
* Correspondence: swb1123@163.com (W. Shi); lhengzzt@bit.edu.cn (H. Liu)

Received: Feb 4, 2022; **Accepted:** Mar 4, 2022; **Published:** Mar 30, 2022

Abstract: Biological signals, such as EEG and ECG, generate complex fluctuations in correspondence with the underlying system dynamics. In this study, we propose a dissimilarity quantification, which is an improvement of information-based similarity for capturing the features of underlying dynamics from positivity or negativity trials in the neurofeedback training of chronic stroke patients. Simulated Gaussian white and pink noises are used to evaluate the validity of this measure by different embedding dimensions, time delays, and data lengths. Then, the method is applied to slow cortical potentials of chronic stroke patients. The results imply that the proposed dissimilarity measure characterizes the unique dynamical patterns of SCP signals. The dissimilarity measure is capable of capturing the underlying dynamics of SCPs that belong to positivity or negativity trials. Besides, as the session progressed, the dissimilarity showed an increasing trend.

Keywords: Information-based similarity, Ordinal pattern, Stroke, Slow Cortical Potentials.

1. Introduction

Non-invasive electroencephalographic (EEG) based brain-computer interface (BCI) is proven to be potential for supporting neuronal plasticity of sub-acute or chronic stroke patients [1–3]. A number of randomized controlled trials have shown positive effects on neurofeedback training programs [4,5]. Yet, there are still important problems that remain unsolved in the implementation of BCI-based rehabilitation in clinical practice. This requires interdisciplinary solutions.

From the methods of EEG neurofeedback, slow cortical potential (SCP) is a classical one. SCP is a cortical polarization measurement from any position on the scalp (preferably the frontocentral region) with a direct current amplifier for more than 0.5–10.0 s. The training of SCP is aiming of modulating specific event-related potentials, in which negative potentials represent an increase in the excitation of underlying neuronal tissue, and positive potentials indicate the level of local cortical arousal and attention. The purpose of such training is to improve the self-regulation capabilities of SCP to improve the regulation ability of cortical excitability to a certain extent [6].

The first successful application of SCP in BCI communication is for locked-in syndrome patients to select letters on a computer screen [7]. From then on, a series of researches have shown that SCP can be used for controlling external devices [8–10]. For example, the patient in the locked-in state was trained to control his SCP and experienced a brainstem stroke [11]. In another study, SCP with negative polarity was successfully used to detect the preparation of lower limb movement [12]. SCP is also an effective and standardized neurofeedback training method to solve the behavioral and neurophysiological defects of ADHD [13]. Besides, SCP neurofeedback training has also been selected as a test method for chronic stroke patients [14].

For the analysis of SCP signals in neurofeedback training, regulating the amplitude changes in SCP is the most intuitive way [15]. Besides, methods based on neural networks have the potential for brain activity classification, too. Altan et al. proposed to use a deep belief network for assessing the clinical usefulness of SCP training in stroke patients in this respect [14]. The statistical methods were combined with the EEG power spectrum and applied to BCI studies in stroke rehabilitation by translating brain signals into predetermined movements of paralyzed limbs [16]. However, the real EEGs are nonstationary, nonlinear, and usually carry noises. Studies have demonstrated that signals such as EEGs generate complex fluctuations which are in correspond with the underlying system dynamics [17–20]. Therefore, feature extraction algorithms of SCPs for neurofeedback training are in pressing demand, especially in the rapid development of BCI.

Information-based similarity (IBS) is a novel method originally proposed for human linguistic style classification based on word order frequency statistics and phylogenetic tree construction [21]. After identifying Shakespeare's works [21], IBS has been successfully applied in detecting the repetition of some basic patterns embedded in human heart rate time series [22–24], human

DNA database [24], blood pressure signals [25], and laser speckle contrast imaging [26]. For these types of signals, the word rank is obtained by mapping the original sequence to a binary sequence, where the increase and decrease of the raw data are referred to as 1 and 0, respectively. However, one essential nature of brain activities is fast oscillatory and multi-sourcing interactions. Selecting a symbolic representation of an ordinal pattern instead of the binary sequence is more appropriate for SCP analysis in BCI studies. In this work, we present an ordinal dissimilarity that is based on the IBS method and apply it in the neurofeedback training from SCP signals in stroke.

2. Materials and Methods

Information-based similarity (IBS) is an algorithm for measuring the dissimilarity between two symbolic sequences [24,27], used for text classification [21,28]. The basic idea of this method is to quantify the differences in repetition patterns between two symbolic signals. In this study, the EEGs were mapped to symbolic sequences based on their corresponding ordinal patterns.

For a given time series $\{x_i; i = 1, 2, \ldots, N\}$, state vectors $X_t = \{x_t, x_{t+\delta}, x_{t+2\delta}, \ldots, x_{t+(m-1)\delta}\}$ are constructed in a m-dimensional space, where m is the length of each reconstructed phase space, $t = 1, 2, \ldots, N - (m - 1)\delta$, and δ is termed as time delay. For each state vector, the series is sorted in a non-decreasing order in which the indices $r_0, r_1, \ldots, r_{m-1}$ correspond to $x_{t+r_0} \le x_{t+r_1} \le \cdots \le x_{t+r_{m-1}}$. The corresponding m-tuple $\pi = (r_0, r_1, \ldots, r_{m-1})$ is the symbolic representation of the state vector and is named a permutation. In this way, the state vector set $\{0, 1, \ldots, m - 1\}$ contains $m!$ possible permutations.

Applying the above procedures, the original time series $\{x_i; i = 1, 2, \ldots, N\}$ can be mapped to a new symbolic series $\{\pi_{m,\delta}(t)\}$ constituted of ordinal patterns π_k ($k = 1, \ldots, m!$), which denotes a unique pattern of fluctuations for a given time series. Fig. 1 illustrates the mapping procedure for 3-dimensional space and time delay equals 1 from a part of the EEG sequence. For $m = 3$, there are a total of 6 (3!) possible ordinal patterns, but there exist 5 ordinal patterns in this example, so the pattern 312 did not show out. This phenomenon is related to the existence of forbidden ordinal patterns in the chaotic dynamics that are ordinary in several chaotic maps [29,30]. These forbidden ordinal patterns can also appear in EEGs corresponding to the signal length and the pattern dimensions [31]. Thus, the number of forbidden ordinal patterns decreases with the signal length, however, increases with the pattern dimension.

For $m = 3$, $\delta = 1$
$\boldsymbol{\pi_k}$: 321, 213, 123, 123, 123, 123, 132, 321, 321, 321, 321, 213, 132, 321, 321, 231, 123

Fig. 1. The mapping procedure for ordinal pattern $m = 3$ and $\delta = 1$.

The probability of each permutation π_k ($k = 1, \ldots, m!$) is defined as

$$p_k(\pi_k) = \frac{\text{the number of } X_t \text{ that has type } \pi_k}{N - (m-1)\delta} \tag{1}$$

Therefore, the probability distribution $P = \{p_k(\pi_k)\}_{k=1,\ldots m!}$ denotes the odds of finding apart from a time series with a specific order that is a rank-frequency distribution. In this study, the forbidden ordinal patterns are discarded.

The dissimilarity measure is developed on the assumption that the information in a signal is mainly determined by the repetitive ordinal patterns of the underlying dynamics. For the above permutation patterns $\{\pi_{m,\delta}(t)\}$, the occurrence times of each ordinal pattern are counted and sorted according to the relative frequency of its occurrence. In this way, the rank-frequency of each pattern π_k ($k = 1, \ldots, m!$) between two sequences mapped from two-time series may not be equal. The rank order of each ordinal pattern of the first symbolic sequence is plotted against its corresponding rank order of the second symbolic sequence. Thus, each point on the graph represents a segment pattern with its rank order in the first symbolic sequence shown on the horizontal axis, against that order in the second symbolic sequence on the vertical axis. The diagonal line of the identification indicates that the rank order of the two signals is equal. The points around the diagonal line represent the rank orders of two symbolic sequences that are close. Fig. 2(c,d) shows comparisons between EEGs for either two positivity trials or two negativity trials. The average deviation between the order points and the diagonal line is a reflection of the distance between the two symbolic sequences. The greater the distance, the less similarity between the two symbolic sequences (Fig. 2b, comparison between positivity and negativity trials), and, vice versa.

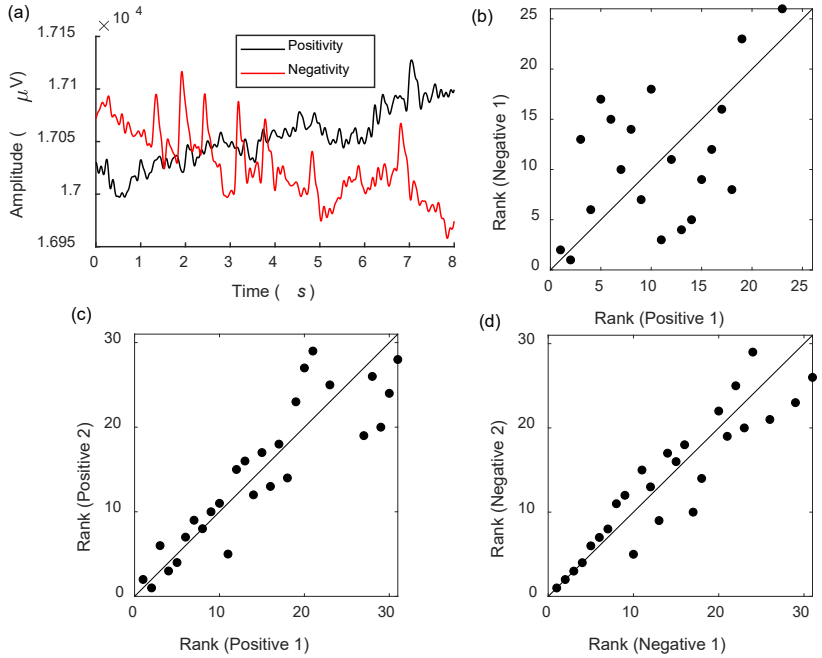

Fig. 2. (a) The plot of a positivity SCP against a negativity SCP of one subject. The detailed data description is introduced in section 4.1. (**b**) Rank order plot of the time series in (**a**), the zero terms are excluded. (**c**) Rank order plot of the SCPs for two positive trials; (**d**) Rank order plot of the SCPS for two negative trials. The black diagonal line is the case where the rank-order of shared patterns for both sequences is identical. The results in (b–d) are for the case $m = 6$, $\delta = 1$.

In order to quantify the similarity between the two sequences more intuitively, a dissimilarity measure is defined according to the rank order of ordinal patterns of two-time series as

$$d_m\left(X_1, X_2\right) = \frac{1}{L}\sum_{k=1}^{L}\left|R_1(\pi_k) - R_2(\pi_k)\right|F(\pi_k) \tag{2}$$

where π_k presents a specific shared ordinal pattern, $R_1(\pi_k)$ and $R_2(\pi_k)$ are the rank order of each π_k in sequences X_1 and X_2, respectively, L is the number of total shared ordinal patterns, and $F(\pi_k)$ is the weight. The greater the d_m is, the farther away from the point from the diagonal line, and the less similar the two sequences are. Clearly, the absolute rank difference, $|R_1(\pi_k) - R_2(\pi_k)|$, represents the absolute distance from a scattered point to the diagonal line. By multiplying a weight function $F(\pi_k)$, which is defined as $F(\pi_k) = \left[-p_1(\pi_k)\log p_1(\pi_k) - p_2(\pi_k)\log p_2(\pi_k)\right]/Z$, differentiated contributions to the overall quantification by various ordinal patterns have been taken into account. $p_1(\pi_k)$ and $p_2(\pi_k)$ in the weight function are the probability of the shared ordinal pattern π_k in sequences X_1 and X_2, separately. Z is the normalization factor defined as $Z = \sum_{k=1}^{L}\left[-p_1(\pi_k)\log p_1(\pi_k) - p_2(\pi_k)\log p_2(\pi_k)\right]$. In this way, the ordinal patterns with higher probabilities become more heavily weighted. The definition of Z is derived from the Shannon entropy, and the latter contains the idea that a specific repetitive pattern is proportional to the total amount of energy represented by the repetitive transitions to the corresponding microstate [24]. Such connection is important since it connects a basic concept of information theory to that of a dynamic system (energy of microstates).

3. Simulation

The Gaussian white noise and the $1/f$ oscillation (pink noise) are applied to examine the effectiveness of the proposed method. To note, the power spectral density of $1/f$ oscillation is inversely proportional to its frequency, which is intrinsically different from white noise. The three interfering factors, data length N, embedding dimension m, and time delay δ of the dissimilarity d_m are discussed in the simulation. For each data length N, 100 realizations are executed. The dissimilarity measure d_m is calculated between Gaussian white noise and the $1/f$ oscillation for each realization.

Fig. 3(a) shows the results of the mean dissimilarity measure between Gaussian white noises and $1/f$ oscillation for different data lengths N. m equals 4, 5, and 6, and time delay δ preserves 1. As shown in the figure, the value of the distance is sensitive to the data length for smaller N, and stables as N grows larger. In addition, for a long enough sequence, the curve of dissimilarity from

m = 4 fluctuates, but with the increase of m, it becomes more stable. As mentioned before, there are m! possible ordinal patterns. The larger the m is, the more potential repetitive patterns can be selected for characterizing the underlying dynamics of time series. Furthermore, the difference between the two signals becomes significant. Thus, the standard deviations for d_m at m = 6 are smaller than in the other two situations. On the other side, there are a total of 24 ordinal patterns at dimension 4, thus shared ordinal patterns may occur in certain distributions by chance.

Fig. 3(b) shows the dissimilarity measure d_m changes with different data lengths N and time delay δ. The dissimilarity d_m is sensitive to the two parameters δ and N when N is relatively smaller. In contrast, the d_m values are more stable for larger N as the probability distribution of ordinal patterns is more statistically characteristic. On the other side, the surface of $d_4(\delta, N)$ oscillate a lot in comparison with that of $d_6(\delta, N)$ even for a larger N. However, the d_6 surface is approximately flat when $N \geq 5000$ no matter what δ equals to. Therefore, the dimension m is chosen as 5 and 6, and time delay δ is set as 1 to decrease fluctuations of the estimates in the following study.

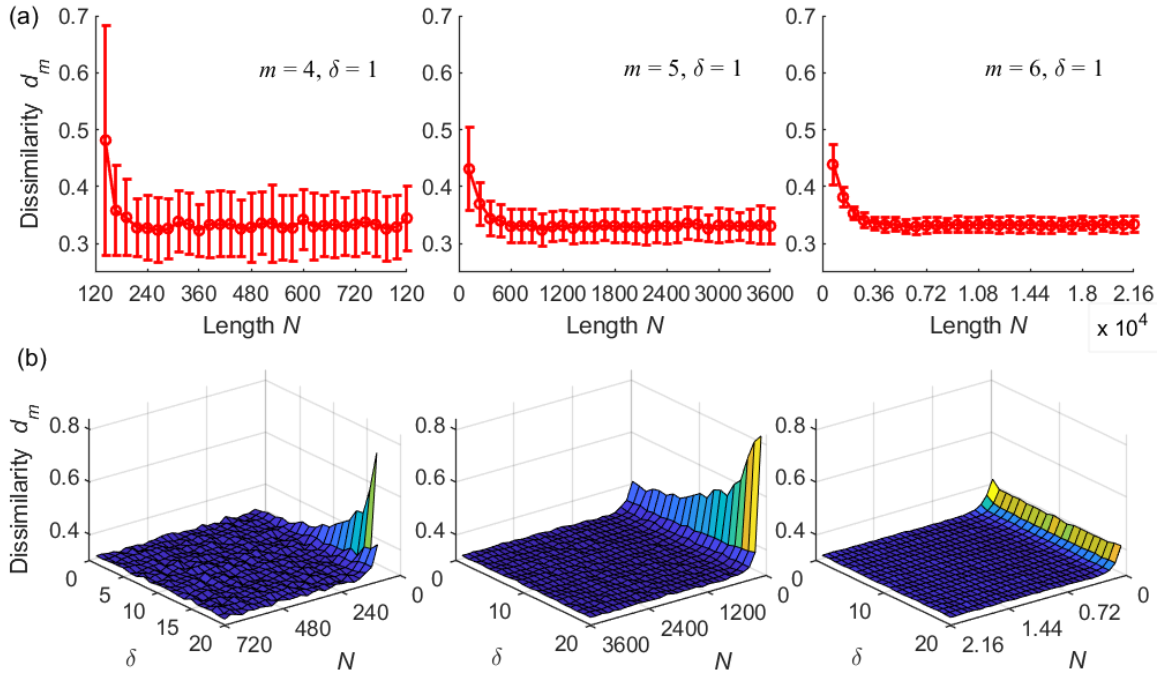

Fig. 3. Dissimilarity results between Gaussian white noise and the 1/*f* oscillation. (**a**) Effect of different series lengths N on dissimilarity measure d_m. Average over 100 realizations for each length N. Circles in the plot represents the mean values and bars represent the standard deviation. (**b**) Effect of different time delay δ on dissimilarity d_m for various length N (72-720) with m = 4 (left), N (120-3600) with m = 5 (medium), and N (720-21600) with m = 6 (right).

4. Applications to SCP Signals in Stroke

4.1. Data Description

The EEG signals were recorded during eight slow cortical potentials (SCP) neurofeedback sessions in two patients with chronic stroke [32]. The interval between two neurofeedback sessions was about one week. The sampling frequency of the recorded EEGs was 256 Hz from the Cz electrode using a Nexus-10 MKII DC amplifier (Mindmedia, Herten, The Netherlands). Each neurofeedback session included the trials that must increase cortical positive and trials that must increase cortical negative. Each trial lasts 8 s (baseline: 0–2 s, active phase: 2–8 s). The feedback consisted of circles with their size and color indicating whether the subject adjusted the baseline activity successfully. The trials were judged successful if the brain activation was adjusted according to the requirements of the task (whether positive or negative), and the participants were successfully instructed. All EEGs were referenced to the linked mastoids and low pass filtered at 10 Hz. In Sessions 1–3, 250 trials were conducted for the positive as well as the negative trials. In sessions 4–8, 375 trials were conducted for negativity, and 125 trials for positivity. A total number of 8000 trials (500 trials for each session and each patient) with 8 s lengths were segmented.

4.2 Results and Discussion

The ordinal pattern-based IBS was conducted during the SCP neurofeedback sessions. To explore the effectiveness of neurofeedback training quantified by the proposed method on stroke patients, we randomly selected 50 positivity trials and 50 negativity trials from the 500 trials from each session each subject to discuss the effect of session, embed dimension m and time delay δ on the dissimilarity measure d_m. Specifically, d_m is calculated between two positivity trials, two negativity trials, or a positivity trial compared with a negativity trial, respectively.

Fig. 4 shows the averaged dissimilarity measure d_m for the first subject. In general, the three surfaces in the lower panel look more similar and have larger values than those in the upper panel. As mentioned before, there are $m!$ possible ordinal patterns in total, but certain patterns do not appear for larger dimensions. That is to say, with the increasing of dimension, the number of forbidden patterns is also increasing for signals with limited length. Therefore, the surfaces in the lower panel are not much different as shown in Fig. 5. As the session progresses, the averaged dissimilarity measure d_m for the first subject increases especially for a larger time delay. Besides, the surface of two negative trials (N&N, when m = 5, Fig. 4) was statistically lower than the other two surfaces. This indicates that neurofeedback training is effective for the first subject. However, the dissimilarity progress is not obvious for the second subject, although the d_m value increases with session progress for time delay δ = 1. However, the dissimilarity progress is not obvious for the second subject, although the d_m value is also increasing with the session progress for time delay δ = 1 (Fig. 5).

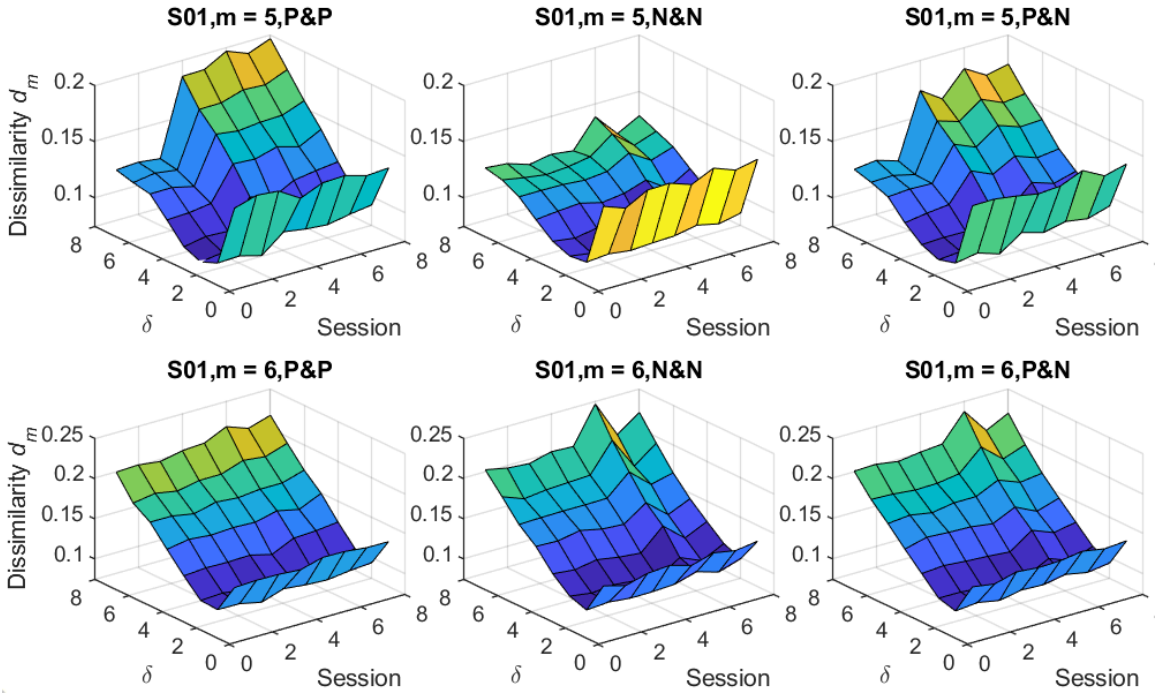

Fig. 4. Averaged dissimilarity dm surface fluctuates with the session progress and time delay δ changing from 1 to 8 for the first subject. The dimension m is set to 5 in the upper panel, and 6 in the lower panel. The left column is the average of 1225 dissimilarities calculated between every two positive trials from the selected 50 positivity trials. Similarly, the middle column is the average of 1225 dissimilarities calculated between every two negative trials from the selected 50 negativity trials. For consistency, 35 positive trials are randomly picked out from the 50 positivity trials and compared to 35 negative trials randomly selected from the 50 negativity trials, and the averaged dm is depicted in the right column.

In addition, with the increasing time delay δ, the averaged dissimilarity measure d_m decreases at first and then increases monotonically for both subjects. For a detailed observation of dissimilarity measures on session progress under different time delays, the plots of d_m with the session under different time delays are shown in Fig. 6. For δ = 1, the d_m plot is flat, but the value is large, and it is difficult to distinguish the three curves. With the increase of δ, the difference between curves gets bigger and bigger, and they are increasing with the session progress. This reflects the positive effect of neurofeedback training on this stroke patient.

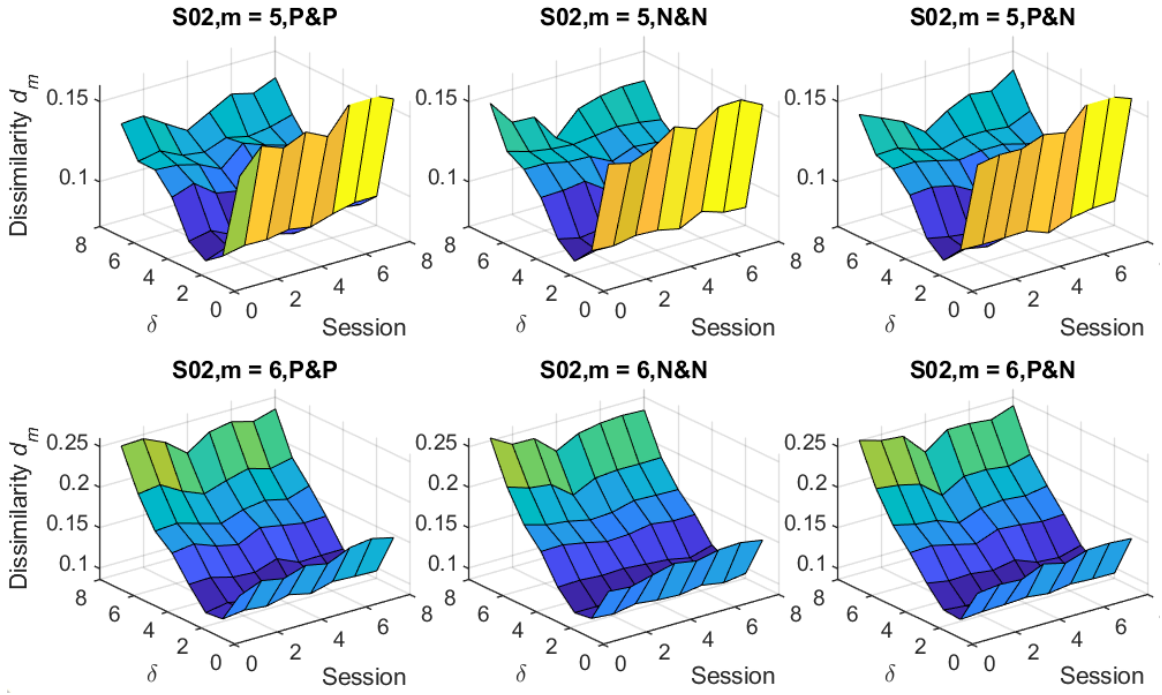

Fig. 5. Effect of different time delay δ on dissimilarity d_m for different sessions for the second subject. The experimental design is the same as Fig. 4.

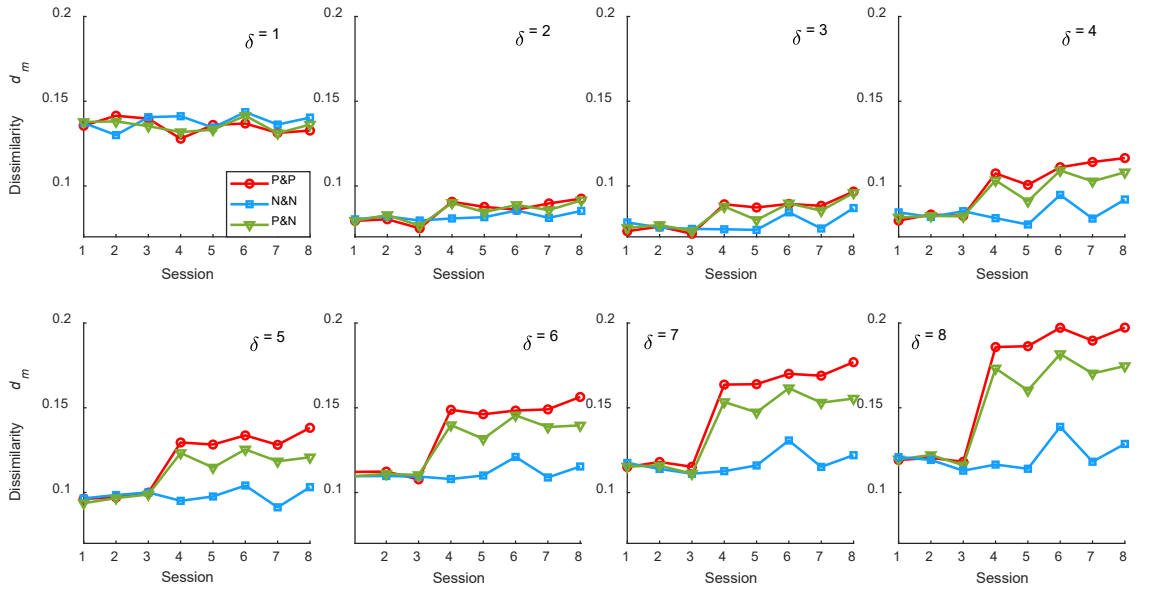

Fig. 6. The effect of session progress on dissimilarity measure d_m for the first subject, the time delay δ changes from 1 to 8, and the plots are averaged results as is shown in Fig. 4.

5. Conclusions

In this study, a method of quantifying the degree of dissimilarity between two signals was introduced. After being verified by noise signals, the method was applied to neurofeedback training for chronic stroke patients. The method assumes that the information content carried in time series is characterized by repetitive ordinal patterns. In the influence of ordinal patterns and forbidden patterns, we discarded the forbidden patterns in the calculation of dissimilarity. The effect of different parameters on the defined dissimilarity measure was validated by Gaussian white noise and $1/f$ oscillation. The result shows that the data length sensitively affects the dissimilarity value, thus enough length signal needs to be considered for stable results. In the application of slow cortical potential training for chronic stroke patients, we find that the dynamical patterns of SCP are characterized by the signal ordinal patterns. The

dissimilarity measure d_m is capable of capturing the underlying dynamics of SCPs that belong to positivity or negativity trials. This neurofeedback training is effective for chronic stroke patients. In the future, more subjects need to be recruited to further verify the effectiveness of this dissimilarity measure in the neurofeedback training of chronic stroke patients.

Author Contributions: Conceptualization, W.S.; Methodology, W.S. and H.L.; Software, C.Z; Validation, C.Z., W.S. and C.-H.Y.; Formal analysis, C.Z. and W.S.; Writing—original draft preparation, W.S. and C.Z.; Writing—review and editing, W.S., C,-H.Y. and H.L.; Visualization, W.S. and C.Z.; Supervision, W.S., C.-H.Y. and H.L.

Funding: This research did not receive external funding.

Acknowledgments: This study is supported by the National Natural Science Foundation of China (Nos. 62001026, 62171028, 61971036, and 61971038).

Conflicts of Interest: The authors declare no conflict of interest.

References

1. Daly, J.J.; Cheng, R.; Rogers, J.; Litinas, K.; et al. Feasibility of a new application of noninvasive brain computer interface (BCI): a case study of training for recovery of volitional motor control after stroke. *Journal of Neurologic Physical Therapy* **2009**, *33*(4), 203–211.
2. Mrachacz-Kersting, N.; Jiang, N.; Stevenson, A.J.T.; Niazi, I.K.; et al. Efficient neuroplasticity induction in chronic stroke patients by an associative brain-computer interface. *Journal of Neurophysiology* **2015**, *115*(3), 1410–1421.
3. Ang, K.K.; Guan, C.; Phua, K.S.; Wang, C.; et al. Brain-computer interface-based robotic end effector system for wrist and hand rehabilitation: results of a three-armed randomized controlled trial for chronic stroke. *Frontiers in Neuroengineering* **2014**, *7*, 30.
4. Toppi, J.; Mattia, D.; Anzolin, A.; Risetti, M.; et al. Time varying effective connectivity for describing brain network changes induced by a memory rehabilitation treatment. In Proceedings of the 36th Annual International Conference of the IEEE Engineering in Medicine and Biology Society, 2014, pp. 6786–6789.
5. Shindo, K.; Kawashima, K.; Ushiba, J.; Ota, N.; et al. Effects of neurofeedback training with an electroencephalogram-based brain–computer interface for hand paralysis in patients with chronic stroke: a preliminary case series study. *Journal of Rehabilitation Medicine* **2011**, *43*(10), 951–957.
6. Omejc, N.; Rojc, B.; Battaglini, P.P.; Marusic, U. Review of the therapeutic neurofeedback method using electroencephalography: EEG Neurofeedback. *Bosnian Journal of Basic Medical Sciences* **2019**, *19*(3), 213–220
7. Chaudhary, U.; Birbaumer, N.; Ramos-Murguialday, A. Brain-computer interfaces for communication and rehabilitation. *Nature Reviews Neurology* **2016**, *12*(9), 513.
8. Birbaumer, N.; Hinterberger, T.; Kübler, A.; Neumann, N. The thought-translation device (TTD): neurobehavioral mechanisms and clinical outcome. *IEEE Transactions on Neural Systems and Rehabilitation Engineering* **2003**, *11*(2), 120–123.
9. Birbaumer, N.; Ghanayim, N.; Hinterberger, T.; et al. A spelling device for the paralysed. *Nature* **1999**, *398*, 297–298.
10. Kübler, A.; Birbaumer, N. Brain-computer interfaces and communication in paralysis: extinction of goal directed thinking in completely paralysed patients? *Clinical Neurophysiology* **2008**, *119*(11), 2658–2666.
11. Chaudhary, U.; Birbaumer, N. Communication in locked-in state after brainstem stroke: a brain-computer-interface approach. *Annals of Translational Medicine* **2015**, *3*.
12. Jiang, N.; Gizzi, L.; Mrachacz-Kersting, N.; Dremstrup, K.; Farina, D. A brain-computer interface for single-trial detection of gait initiation from movement related cortical potentials. *Clinical Neurophysiology* **2015**, *126*(1), 154–159.
13. Mayer, K.; Wyckoff, S.N.; Strehl, U. One size fits all? Slow cortical potentials neurofeedback: a review. *Journal of Attention Disorders* **2013**, *17*(5), 393–409.
14. Altan, G.; Kutlu, Y.; Allahverdi, N. Deep Belief Networks Based Brain Activity Classification Using EEG from Slow Cortical Potentials in Stroke. *International Journal of Applied Mathematics, Electronics and Computers* **2016**, *4*, 205–210.
15. Pichiorri, F.; Mrachacz-Kersting, N.; Molinari, M.; Kleih, S.; Kübler, A.; Mattia, D. Brain-computer interface based motor and cognitive rehabilitation after stroke-state of the art, opportunity, and barriers: summary of the BCI Meeting 2016 in Asilomar. *Brain-Computer Interfaces* **2017**, *4*(1–2), 53–59.
16. Biasiucci, A.; Leeb, R.; Iturrate, I.; et al. Brain-actuated functional electrical stimulation elicits lasting arm motor recovery after stroke. *Nature Communications* **2018**, *9*(1), 2421.
17. Shi, W.; Yeh, C.; An, J. Cross-Channel Phase-Amplitude Transfer Entropy Conceptualize Long-Range Transmission in sleep: a case study. In Proceedings of the 41st Annual International Conference of the IEEE Engineering in Medicine and Biology Society (EMBC), 2019, pp. 4048–4051.
18. Shi, W.; Yeh, C.; Hong, Y. Cross-Frequency Transfer Entropy Characterize Coupling of Interacting Nonlinear Oscillators in Complex Systems. *IEEE Transactions on Biomedical Engineering* **2018**, *66* (2), 521–529.

19. Yeh, C.; Shi, W. Generalized multiscale Lempel-Ziv complexity of cyclic alternating pattern during sleep. *Nonlinear Dynamics* **2018**, *93*(4), 1899–1910.
20. Yeh, C.-H.; Shi, W. Identifying phase-amplitude coupling in cyclic alternating pattern using masking signals. *Scientific Reports* **2018**, *8* (1), 2649.
21. Yang, A.C.C.; Peng, C.K.; Yien, H.W.; Goldberger, A.L. Information categorization approach to literary authorship disputes. *Physica A: Statistical Mechanics and its Applications* **2003**, *329*(3–4), 473–483.
22. Cui, X.; Chang, E.; Yang, W.H.; Jiang, B.C.; Yang, A.C.C.; Peng, C.K. Automated detection of paroxysmal atrial fibrillation using an information-based similarity approach. *Entropy* **2017**, *19*(12), 677.
23. Yang, A.C.; Tsai, S.J.; Hong, C.J.; et al. Clustering heart rate dynamics is associated with β-adrenergic receptor polymorphisms: analysis by information-based similarity index. *PloS One* **2011**, *6*(5), e19232.
24. Peng, C.K.; Yang, A.C.; Goldberger, A.L. Statistical physics approach to categorize biologic signals: from heart rate dynamics to DNA sequences. *Chaos: An Interdisciplinary Journal of Nonlinear Science* **2007**, *17*(1), 015115.
25. Yeh, J.R.; Lin, T.Y.; Shieh, J.S.; Chen, Y.; Peng, C.K. A novel blocking index based on similarity measurement applied in distinguishing the patterns of blood pressure signals at dynamically transitional situation. *Biomedical Engineering: Applications, Basis and Communications* **2008**, *20*(2), 107–114.
26. Humeau-Heurtier, A.; Abraham, P.; Mahé, G. Linguistic analysis of laser speckle contrast images recorded at rest and during biological zero: comparison with laser Doppler flowmetry data. *IEEE Transactions on Medical Imaging* **2013**, *32*(12), 2311–2321.
27. Yang, A.C.; Goldberger, A.L.; Peng, C.K. Genomic classification using an information-based similarity index: application to the SARS coronavirus. *Journal of Computational Biology* **2005**, *12*(8), 1103–1116.
28. Yang, A.C.; Hseu, S.S.; Yien, H.W.; Goldberger, A.L.; Peng, C.K. Linguistic analysis of the human heartbeat using frequency and rank order statistics. *Physical Review Letters* **2003**, *90*, 108103.
29. Amigó, J.M.; Kocarev, L.; Szczepanski, J. Order patterns and chaos. *Physics Letters A* **2006**, *355*(1), 27–31.
30. Ribeiro, H.V.; Jauregui, M.; Zunino, L.; Lenzi, E.K. Characterizing time series via complexity-entropy curves. *Physical Review E* **2017**, *95*(6), 062106.
31. Yeh, C.; Fang, Y.; Shi, W.; Hong, Y. A novel method of visualizing q-complexity-entropy curve in the multiscale fashion. *Nonlinear Dynamics* **2019**, *97*(4), 2813–2828.
32. Ruben, R.; Helena, E.; Andreas, H.; Teresa, S.; Andrea, K.; Sonja, C.K. *Slow Cortical Potential Training in Stroke*; 2014. (In Germany)

Publisher's Note: IIKII stays neutral with regard to jurisdictional claims in published maps and institutional affiliations.

Copyright: © 2022 The Author(s). Published with license by IIKII, Singapore. This is an Open Access article distributed under the terms of the Creative Commons Attribution License (CC BY), which permits unrestricted use, distribution, and reproduction in any medium, provided the original author and source are credited.